

Optimization of Conditions for the synthesis of new Triphenylphosphonium-Substituted phthalocyanine from Tetrabrominated Phthalocyanine using Experimental Design Method

Mohamed Tarhouni^{1,2,3}, Bassem Jamoussi³

¹Chemistry Department, Gebze Technical University, Gebze, 41400 Kocaeli, Turkey

²Faculté Des Sciences de Bizerte, Université de Carthage, UR17ES01 Didactique des Sciences Expérimentales et de chimie supramoléculaire, 7021 Zarzouna Bizerte, Tunisia

³Université Virtuelle de Tunis, UR17ES01 Didactique des Sciences Expérimentales et de Chimie Supramoléculaire, Tunis, Tunisia

Abstract: An experimental design has been drawn up to optimize the experimental conditions of the synthesis of new Triphenylphosphonium-substituted phthalocyanine from tetrabrominated phthalocyanine. Response surface methodology (RSM) was applied to study the influence of molar ratio of tetrabrominated phthalocyanine to triphenylphosphine, reaction time and the reaction temperature. Quadratic model was developed for yield of Triphenylphosphonium-substituted phthalocyanine using Design-Expert software NEMRODW. The model was used to calculate the optimum operating conditions for synthesis of Triphenylphosphonium-substituted phthalocyanine. The optimum conditions were obtained as follows: n (tetrabrominated phthalocyanine TTBPc) : n (triphenylphosphine PPh₃) = 1:20, reaction time 12 h and reaction temperature 120°C. Under these conditions, the yield of Triphenylphosphonium-substituted phthalocyanine reached 70%

Keywords: Triphenylphosphonium-substituted phthalocyanine; tetrabrominated phthalocyanine; Response surface methodology

1. Introduction

Phosphonium salts play important role in chemistry, especially as precursors of phosphorus ylides in synthesis of olefins via the Wittig-reaction [1, 2]. In most cases the required phosphonium salts are obtained from triphenylphosphane by heating it with the appropriate alkyl or benzyl halide in dry solvents.

For many years Arylphosphonium salts are compounds that have both lipophilic and cationic character, allowing a facile transport through plasma membranes or cell walls. The nature of the mitochondrial membrane is prone to interact with positively-charged and lipophilic molecules. Recently, much attention has been directed towards targeting bioactive compounds to cell mitochondria, in order to remediate mitochondrial dysfunctions that are the cause of a number of diseases, including cancer [4, 5].

One approach typically employed to target drugs to mitochondria is to conjugate the bioactive molecule of choice directly to mitochondriotropic ligands such as the triphenylphosphonium group (TPP) [6, 7]. So labelling and imaging of mitochondria is an important aspect for understanding the cellular processes and in vitro diagnostic assay. [8-15] Mitochondria targeting is also considered as therapeutic strategy for cancer [12] that involves their destruction via delivering drugs/nanomaterials followed by therapy. [16] for specific targeting of mitochondria.

Among them triphenylphosphonium (TPP) is widely used for mitochondria targeting. [8, 9] TPP is a polar cationic molecule with high lipophilicity which makes it suitable for

penetrating the mitochondrial intermembrane potential barrier and have been used in different mitochondria targeting materials. [8, 9] TPP has been conjugated with nanoparticle, [17-19] dendrimer, [13] liposome [12] and reported for targeted drug delivery and imaging of mitochondria.

Mitochondrial targeting, in particular, now attracts increasing attention for subcellular targeting [20-21] is starting to be applied to PDT. The synthesis of a new family of Triphenylphosphonium-substituted with positively Phthalocyanines (Pcs) are gathering importance as effective photosensitizers in targeted PDT and imaging of tumors.

This work is a complement and a very large extension of the work we have previously reported concerning Biological activities on human cancer cells of Triphenylphosphonium-substituted phthalocyanine [22] by employing a rational approach to maximize the reaction yield of the desired product. Furthermore, a surface response methodology (RSM) approach was used to statistically identify critical reaction parameters with high yield.

The preparation of Triphenylphosphonium-substituted Phthalocyanines (Pcs) is influenced by many factors. For this reason a preliminary study on the effect of these factors on the preparation was carried out in order to determine the most important ones and their regions of interest. The most influential factors were found to be reaction time (X1), PPh₃ to TTBPc molar ration (X2) and reaction temperature (X3). Thus, in the present work, we synthesized Zn (II) phthalocyanine core with triphenylphosphonium units by reacting triphenylphosphine with halogenoalkanes (scheme

1) [22] with values of (X1), (X2) and (X3) included in the suitable range. Desirable preparation outputs based on reaction yield (Y) was considered as responses. Thus, an experimental design methodology is applied to relate the experimental conditions of the Synthetic route of Zn (II) phthalocyanine core with triphenylphosphonium units with high percent yield. Furthermore, response surface methodology (RSM), an efficiently statistical technique, was applied to determine the optimum operating conditions with minimum number of experiments.

2. Materials and Methods

All solvents and reagents were of reagent grade quality and obtained commercially from Aldrich, Fluka or Merck. FT-IR spectra were recorded between 4000 and 650 cm⁻¹ using a PerkinElmer Spectrum 100 FT-IR spectrometer. NMR spectra were recorded in deuterated solvents on a Varian 500 MHz spectrometer at 298 K. 31P NMR spectrum was

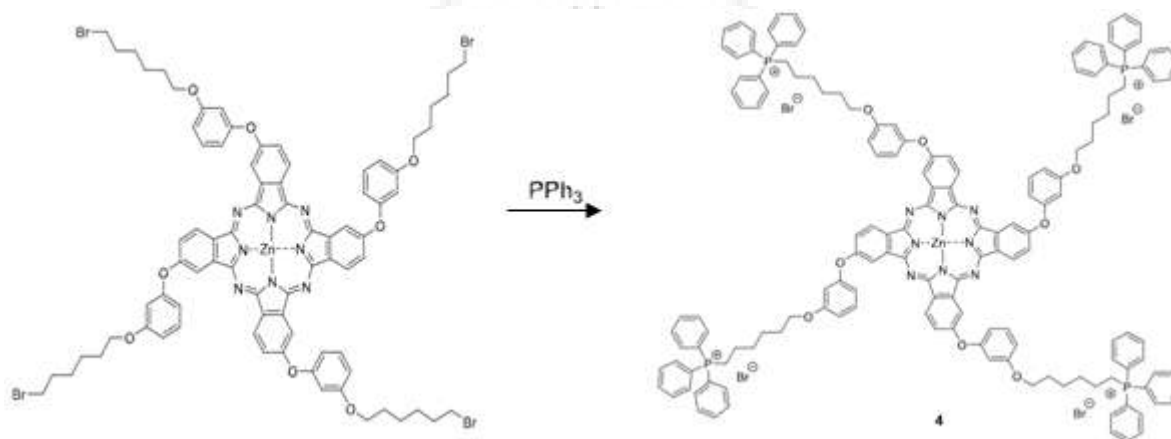
recorded with a 202.26 MHz magnetic field, in proton-decoupling conditions. Mass spectra were recorded on a MALDI (matrix assisted laser desorption ionization) BRUKER Microflex LT.

Phthalocyanine bearing Triphenylphosphonium-functions was prepared as reported [22].

Synthesis of Triphenylphosphonium-substituted Zn (II) phthalocyanine and characterization

The Zn (II) phthalocyanine core with triphenylphosphonium units was synthesized using a procedure **previously described** by Tarhouni and coworkers [22]. All classical analyses (FT-IR, MS-MALDI-TOF, 1H and 31P NMR) have been performed and confirmed the proposed structure.

The formation of **Triphenylphosphonium-substituted Zn (II) phthalocyanine** reaction undergoes based on the following reaction:



Scheme 1: Synthetic route of Zn (II) phthalocyanine core with triphenylphosphonium units

3. Experimental Design and Mathematical Model

Central composite design

RSM was a collection of mathematical and statistical techniques that was utilized to design experiments, build models and analyze the effects of the several independent variables. RSM was an effective tool to study the individual and interactive effects of these factors in order to find the target value [23-27].

The Box-Behnken experimental design was chosen to study the combined effects of reaction time, PPh3 to TTBPc molar ratio and reaction temperature (on the yield of phthalocyanine by RSM). The experimental design was carried out by three chosen independent process variables at three levels including reaction time (x_1), PPh3/ TTBPc mole ratio (x_2) and temperature (x_3) shown in Table 1.

Table 1: Parameter levels and coded values in the experimental design

Factor	Symbol	Range and level		
		-1	0	1
Reaction time/h	X1	4	8	12
PPh3/TTBPc	X2	10	20	30
Reaction temperature °C	X3	80	120	160

A 2³ full-factorial Box-Behnken experimental design with coded levels augmented by 2*3 axial points ($\pm\alpha, 0, 0$), ($0, \pm\alpha, 0$), ($0, 0, \pm\alpha$), and 2c center points (0, 0, 0) [13-14]. Hence, the total number of tests (N) required for the three independent variables is:

$$N = 2^3 + (2 \times 3) + 2 = 16.$$

The center points are made up of all variables at zero level which are crucial in determination of experimental error and the reproducibility of the data. On the other hand, combination of variables consisting of one at its lowest (-a) level or highest (a) level with other variables at zero level constitutes the axial points. a is the distance of the axial point from center and makes the design rotatable and is calculated by $a = 2n/4$, where n is the factor numbers (in this study, three factors are being evaluated, so a is equal to 1.68).

Replicates of the test at the center are very important as they provide an independent estimate. Variables were designed at levels by associated plus signs (+1) with high levels, zero (0) indicating center value and minus signs (-1) with low levels. The coded values of these factors were obtained according to equation 1 as follows:

$$x_i = \frac{X_i - X_0}{\Delta X_i}$$

where x_i was the independent variable coded value, X_i was the independent variable real value, X_0 was the independent variable real value at the center point, and ΔX_i was (variable at high level-variable at low level)/2. The independent variables and their levels, real values are presented in Table1.

The second-order model was performed to predict the optimum value and correlate the response variable to the independent variable. The quadratic equation model was described according to equation 2 :

$$Y = \beta_0 + \sum_{i=1}^3 \beta_{ii}X_i^2 + \sum_{i=1}^3 \sum_{j=1}^3 \beta_{ij}X_iX_j$$

where Y was the predicted response, x_i and x_j were the coded levels of the independent variables, β_0 was the center point of the system, β_i , β_{ii} , β_{ij} were the linear terms, the squared terms for the variable i , and the interaction terms between variables i and j , respectively.

The responses and the corresponding parameters are modeled and optimized using ANOVA to estimate the statistical parameters by means of response surface methods.

RSM differs from classical experimental procedures, considered the effect of factors and their interactions involved to reduce the number of cumbersome experiments and get the optimal conditions. [28] Independent variables and their levels for the Box-Behnken design used in this study are shown in Table 1. To verify the models, 16 runs of experiment were conducted and the obtained response values are shown in Table2. It could be seen that the experimental values and calculated values had no observable difference.

Table 2: Experimental design and response value

Experimental No.	Reaction time / h	PPh3/TTBPC	Reaction Temperature	Yield of Reaction / %	
				Expt	Calc.
1	-1	-1	-1	42.03	43.507
2	1	-1	-1	57.3	57.247
3	-1	1	-1	54.76	59.525
4	1	1	-1	45.78	55.13
5	-1	-1	1	40.49	43.07
6	1	-1	1	50.49	55.861
7	-1	1	1	55.56	92.48
8	1	1	1	44.18	82.6
9	-α	0	0	63.58	67.9
10	+α	0	0	65.42	60.34
11	0	-α	0	52.58	61.75
12	0	+α	0	52.23	48.02
13	0	0	-α	63.9	65.67
14	0	0	+α	59.78	60.81
15	0	0	0	63.89	63.24
16	0	0	0	62.91	63.24

The predicted quadratic model related the yield of **Zn (II) phthalocyanine core with triphenylphosphonium units** with three independent factors (reaction time, **PPh3/TTBPC** molar ratio, **reaction Temperature**) was expressed in equation 3 as follows:

$$Y = 63.242 + 0.420X_1 + 0.807X_2 - 1.445X_3 - 0.776X_1X_1 - 11.188X_2X_2 - 2.476X_3X_3 - 5.663X_1X_2 - 0.787 X_1X_3 + 0.937 X_2X_3$$

where x_1 , x_2 and x_3 were the coded values of the best variables reaction time, **PPh3/TTBPC** molar ratio and **reaction Temperature**, respectively; Y was the response of yield of **Zn (II) phthalocyanine core with triphenylphosphonium units**.

Positive sign in front of the terms indicates synergistic effect, whereas negative sign indicates antagonistic effect. The coefficient of the model for the response was estimated using multiple regression analysis technique included in the RSM. Fit quality of the models was judged from their coefficients of correlation and determination.

Table3. Analysis of variance (ANOVA) for response surface quadratic model for

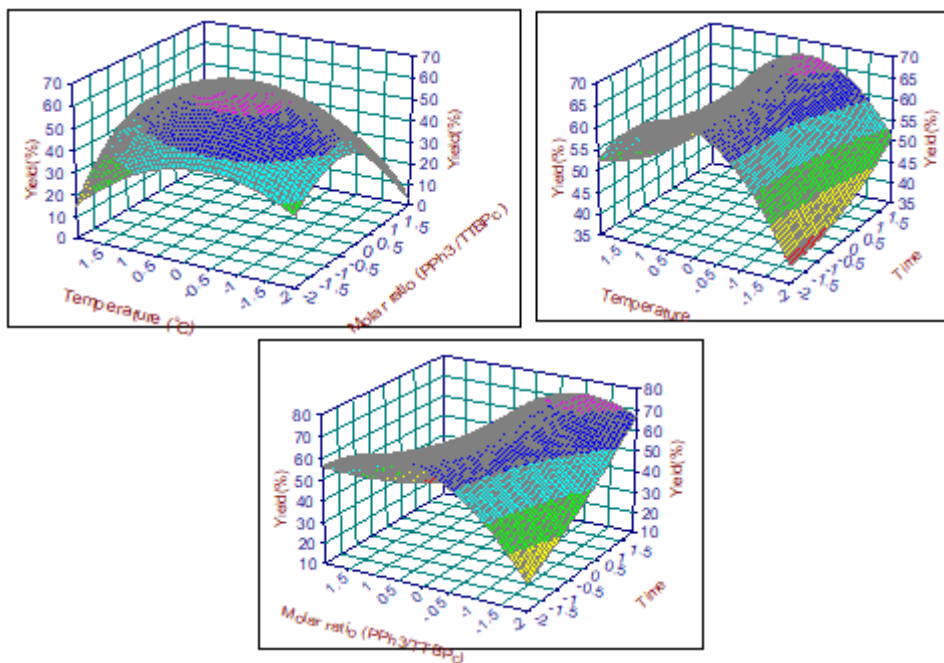
Zn (II) phthalocyanine core with triphenylphosphonium units

Source of variation	Sum of squares	Degree of freedom	Mean square	Fexp	Signif
Regression	926.3612	9	102.9290	53.3368	0.0176***
Residual	11.5788	6	1.9298		
Lack of fit	11.4775	5	2.2955	22.6716	16.5
Pure error	0.1013	1	0.1013		
Correlation total	937.9400	15			

***Significant at 99.9% level confidence

The parameter levels and coded values were given in table 2. The graphical representations of the distribution of these experimental points are given in Fig. 1. The measured responses are defined as Reaction yield in %.

Figure 1 Response surface plots showing the predicted values of yield of **Zn (II) phthalocyanine core with triphenylphosphonium units**, (a) effect of reaction temperature and PPh3/TTBPC molar ratio (b) reaction time and reaction temperature, (c) reaction time and PPh3/TTBPC molar ratio.



Model fitting and statistical analysis

The statistical software package Design-Expert, NEMRODW, was used for regression analysis of experimental data to fit the equations developed and also to plot response surface. The quality of the developed model can be determined from the value of correlation (R^2) while evaluation of the statistical significance of the equations developed can be determined by using an analysis of variance (ANOVA).

4. Results and Discussion

RSM experiments and studying

Analysis of variance (ANOVA) of the regression model was employed to seek out the significance of the effects of parameters on reaction process (Table 3). The significance of regression model was examined by F -test and p -value. As shown in (Table 3), the computed F -value (53.33) was much larger than the tabular F -value (3.70), which was desirable as it indicated that the model obtained from equation 3 gave a good prediction at 1% level of significance. In addition, the p -value for the model less than 0.0001 also meant that the model term was significant. In the study, x_1 , x_2 , x_4 , x_1x_3 , x_1x_4 and x_2x_3 were significant factors. Furthermore, the coefficient of determination (R^2) of the model was 0.9016, which implied that 90.16% of the variation could be explained by the fitted model. In general, the quadratic regression model with the R^2 value higher than 0.90 was considered as possessing a considerable high correlation [29, 30]. On investigating R^2 value, the predicted R^2 of 0.7399 was in reasonable agreement with the adjusted R^2 of 0.9016. The adequacy precision of 53.33 was much greater than 4, which indicated that the model could be used to navigate the design space. The desirable results represented that the chosen quadratic model was appropriate in predicting the response variables for the experimental data.

Statistical analysis

The quality of the model developed was evaluated based on the correlation coefficient value. The R^2 values for Eqs 1

was 0.939. Both the R^2 values obtained were relatively high (close to unity), indicating that this was a good agreement between the experimental and the calculated values of the determination coefficients of the multilinear regression from the models.

The adequacy of the models was further justified through analysis of variance (ANOVA). The ANOVA for the quadratic model for yield of **Zn (II) phthalocyanine core with triphenylphosphonium units** yield is listed in TABLE 3.

Reading the data in TABLE 3 reveals the validity of the model since the value of F_{exp} (22.67), which is the ratio between the Lack of fit and the pure error, is much lower than the critical value of Fisher ($F_{0.001}(5,1) = 5764$) at a 99.9% level of confidence with 5 and 1 degrees of freedom.

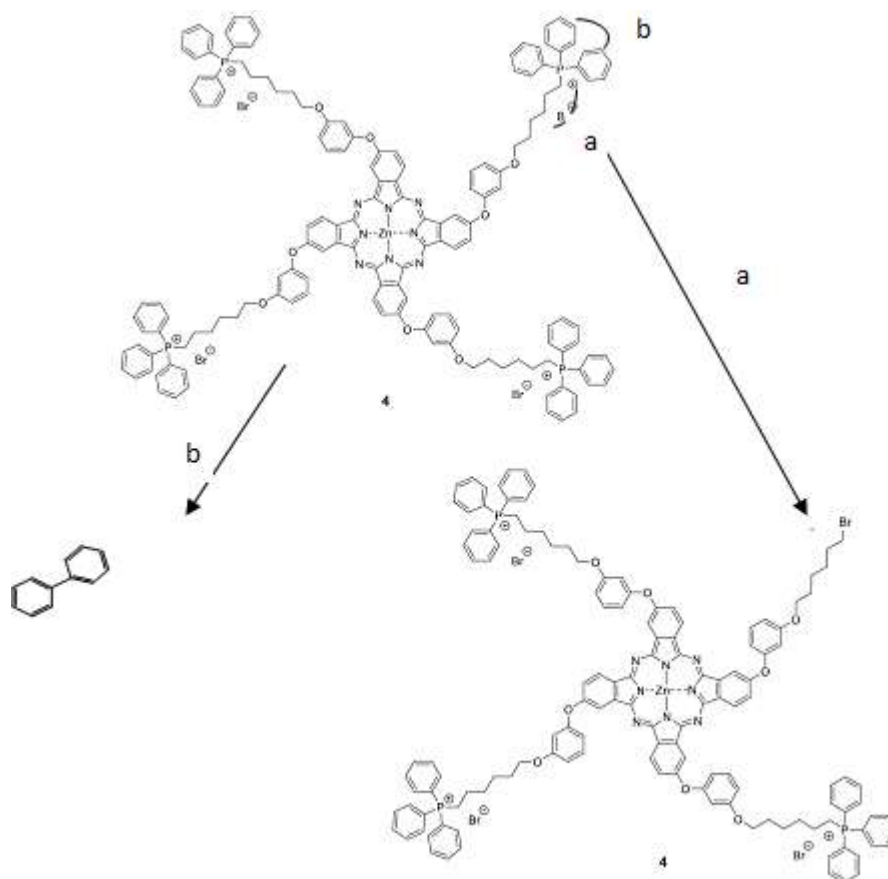
The results of the ANOVA (TABLE 3) also shows that the experimental value of $S_{cnedcor}$ ($F_{exp} = 53, 33$), which is the ratio between the square of the Response surface plots facilitated the interaction study of the process variables for **tetra-triphenylphosphonium phthalocyanine** yield. The three dimensional (3-D) response plots of reaction time, PPh₃/TTBPC molar ratio and reaction temperature are shown in Figure 1.

The variation of yield of **Zn (II) phthalocyanine core with triphenylphosphonium units** with (a) effect of reaction temperature and PPh₃/TTBPC molar ratio was presented in Figure 1- (a) and. The interaction between reaction time and PPh₃/TTBPC molar ratio reaction time is given in Figure 1_ (c). It could be seen that the yield of **Zn (II) phthalocyanine core with triphenylphosphonium** changed little compared to the effect of time. With increasing temperature, the yield increased, passing through a maximum and then decreased slightly. Certainly, the reaction with PPh₃/TTBPC molar could not be conducted at a very high molar ratio. As it could be seen, the yield reached a maximum value around 120°C and then declined

Figure 1- (c) and 1- (a) presented the three dimensional related to yield of **Zn (II) phthalocyanine core with triphenylphosphonium units** as a function of reaction time and amount of PPh₃/TTBPC molar ratio under constant temperature. As it could be seen on the three-dimensional response surface, the yield of **Zn (II) phthalocyanine with triphenylphosphonium** changing slightly to the maximum meant that the reaction time on the response showed a more significant influence in comparison to temperature. With a further increase in temperature, a significant decrease in yield occurred what be explained by decomposition temperature for the phosphonium salt.

The reaction paths of tetraphenylphosphonium de phthalocyanine degradation can be explained by the following assumptions:

At temperatures >160 °C, reaction pathways involving reactive intermediates, namely free radicals, are more probable. Thus, in the case involves the homolysis of the P-phenyl bond to generate triphenylphosphonium radical and phenyl radical, which can subsequently either combine with another phenyl radical to form biphenyl or a bromine atom to form bromoalkyltriphenylphosphonium de phthalocyanine (Scheme2)



Scheme 2: Degradation route of Zn (II) phthalocyanine core with triphenylphosphonium units at temperature higher than 160°C

The yield increased significantly before amount of PPh₃/TTBPC molar ratio reached 20, but insignificant change was observed for molar ratio over 20. Meanwhile, the yield decreased gradually as temperature increased but changed slightly when temperature exceeded 120°C. The saddle shape of the plots showed that the relationships between PPh₃/TTBPC molar ratio and temperature are likely to affect the reaction. The plot indicated that the maximum value (69%) was associated with molar ratio value 20 and temperature 120°C.

Attaining optimum conditions and model verification

Based on the 16 experimental data, the model predicted the optimum yield for **triphenylphosphonium phthalocyanine** of PPh₃ over TTBPc could reach 72%, with the optimal process conditions of reaction time 12 h, alcohol/acid molar ratio 20 and reaction temperature 120°C. In order to verify the adequacy of the model, three parallel experiments were

conducted, under the conditions above and the average yield reached 70.9%, which meant that the predicted and experimental data had a good agreement.

5. Conclusions

The response surface methodology based on Box-Behnken experimental design was employed for optimization the experimental conditions of the synthesis of new Triphenylphosphonium-substituted phthalocyanine from tetrabrominated phthalocyanine

The optimum conditions were obtained as follows: *n* (tetrabrominated phthalocyanine TTBPc): *n* (triphenylphosphinePPh₃) = 1:20, reaction time 12 h and reaction temperature 120°C. Under these conditions, the yield of Triphenylphosphonium-substituted phthalocyanine

reached 70%. in close agreement with values predicted by the mathematical model (97.82%).

References

- [1] Byrne PA, Gilheany D (2013) Chem Soc Rev 42: 6670-6696
- [2] Kolodiazny O. I. (1999) *Phosphorus ylides. Chemistry and applications in organicsynthesis*, Wiley-VCH, Weinheim, Germany
- [3] Wu J, Zhang D, Wei S (2005) Synth Commun 35: 1213-1222
- [4] DiMauro, S. Mitochondrial diseases. Biochim. Biophys. Acta 2004, 1658, 80–88.
- [5] Grabacka, M.M.; Gawin, M.; Pierzchalska, M. Phytochemical Modulators of Mitochondria: The Search for Chemopreventive Agents and Supportive Therapeutics. *Pharmaceuticals* 2014, 7, 913–942.
- [6] Lu, P.; Bruno, B.J.; Rabenau, M.; Lim, C.S. Delivery of drugs and macromolecules to the mitochondria for cancer therapy. *J. Control. Release* 2016, 240, 38–51.
- [7] Cui, H.; Huan, M.; Ye, W.; Liu, D.; Teng, Z.; Mei, Q.-B.; Zhou, S. Mitochondria and Nucleus Dual Delivery System to Overcome DOX Resistance. *Mol. Pharm.* 2017, 14, 746–756.
- [8] Modica-Napolitano, J. S.; Aprile, J. R. Delocalized Lipophilic Cations Selectively Target the Mitochondria of Carcinoma Cells. *Adv. Drug Deliver Rev.* 2001, 49, 63–70.
- [9] Lin, T. K.; Hughes, G.; Muratovska, A.; Blaikie, F. H.; Brookes, P. S.; Darley-Usmar, V.; Smith, R.; Murphy, M. P. Specific Modification of Mitochondrial Protein Thiols in Response to Oxidative Stress. *J. Biol. Chem.* 2002, 277, 17048–17056.
- [10] Zhou, Y.; Liu, S. 64Cu-Labeled Phosphonium Cations as PET Radiotracers for Tumor Imaging. *Bioconjugate Chem.* 2011, 22, 1459–1472.
- [11] Zhao, N.; Li, M.; Yan, Y. L.; Lam, J. W. Y.; Zhang, Y. L.; Zhao, Y. S.; Wong, K. S.; Tang, B. Z. A Tetraphenylethene-substituted Pyridinium Salt with Multiple Functionalities: Synthesis, Stimuli-responsive Emission, Optical Waveguide and Specific Mitochondrion Imaging. *J. Mater. Chem. C* 2013, 1, 4640–4646.
- [12] Solomon, M. A.; Shah, A. A.; D'Souza, G. G. M. In Vitro Assessment of the Utility of Stearyl Triphenyl Phosphonium Modified Liposomes in Overcoming the Resistance of Ovarian Carcinoma Ovar-3 Cells to Paclitaxel. *Mitochondrion* 2013, 13, 464–472.
- [13] Wang, X. Y.; Shao, N. M.; Zhang, Q.; Cheng, Y. Y. Mitochondrial Targeting Dendrimer; Allows Efficient and Safe Gene Delivery. *J. Mater. Chem. B* 2014, 2, 2546–2553.
- [14] Ma, X. C.; Wang, X. B.; Zhou, M.; Fei, H. A Mitochondria-Targeting Gold-Peptide Nanoassembly for Enhanced Cancer-Cell Killing. *Adv. Healthcare Mater.* 2013, 2, 1638–1643.
- [15] Leung, C. W. T.; Hong, Y. N.; Chen, S. J.; Zhao, E. G.; Lam, J. W. Y.; Tang, B. Z. A Photostable AIE Luminogen for Specific Mitochondrial Imaging and Tracking. *J. Am. Chem. Soc.* 2013, 135, 62–65
- [16] Ju, E. G.; Li, Z. H.; Liu, Z.; Ren, J. S.; Qu, X. G. Near-Infrared Light-Triggered Drug-Delivery Vehicle for Mitochondria-Targeted Chemo-Photothermal Therapy. *ACS Appl. Mater. Interfaces* 2014, 6, 4364–4370.
- [17] Marrache, S.; Dhar, S. Engineering of Blended Nanoparticle Platform for Delivery of Mitochondria-Acting Therapeutics. *Proc. Natl. Acad. Sci.* 2012, 109, 16288–16293.
- [18] Poly-L-Lysine Assisted Synthesis of Core-Shell Nanoparticles and Conjugation with Triphenylphosphonium to Target Mitochondria. *J. Mater. Chem. B* 2013, 1, 5143–5142.
- [19] Du, F. K.; Min, Y. H.; Zeng, F.; Yu, C. M.; Wu, S. Z. A Targeted and FRET-Based Ratiometric Fluorescent Nanoprobe for Imaging Mitochondrial Hydrogen Peroxide in Living Cells. *Small* 2014, 10, 964–972.
- [20] Denora N, Iacobazzi RM, Natile G and Margiotta N. *Coord. Chem. Rev.* 2017; 341: 1–18.
- [21] Zielonka J, Joseph J, Sikora A, Hardy M, Ouari O, Vasquez-Vivar J, Cheng G, Lopez M and Kalyanaraman B. *Chem. Rev.* 2017; 117: 10043–10120
- [22] Mohamed Tarhouni, Denis Durand, Emel Önal, Dina Aggadd, Ümit İ-s, Gülçin Ekineker, Frédérique Brégierc, Bassem Jamoussi, Vincent Solc, Magali Gary-Bobod and Fabienne Dumoulina
- [23] Sarra Bouazizi, Bassem Jamoussi and Dalila Bousta ; *International Journal of Engineering Research & Technology*, Vol.5 Issue 05, May 2016, p32-41
- [24] Nouredine Elboughdiri ; Ammar Mahjoubi ; Ali Shawabkeh ; Hussam Khasawneh ; Bassem Jamoussi ; May 2015; *Advances in Chemical Engineering and Science* 5:111-120
- [25] Manel Baizig ; Bassem Jamoussi; Narjes Batis 3- May 2013; *Water Quality Research Journal of Canada*
- [26] Ines Missaoui ; Lotfi Sayadi ; Bassem Jamoussi ; Bechir Ben Hassine ; 2009 ; *Journal of chromatographic science* 47 (4):257-62
- [27] A. H. Hamzaoui ; Bassem Jamoussi ; M'nif Adel ; January 2008 *Hydrometallurgy* 90 (1):1-7
- [28] Martendal, E.; Budziak, D.; Carasek, E.; *J. Chromatogr. A* 2007, 1148, 131.
- [29] Li, Y.; Lu, J.; Gu, G. X.; Mao, Z.; *J. Am. Soc. Brew. Chem.* 2005, 63, 171.
- [30] Wu, S. J.; Yu, X.; Hu, Z. H.; Zhang, L. L.; Cheng, J. M.; *J. Environ. Sci.* 2009, 21, 1276.